

Numerical Hydrodynamic Assessment

KIRSTEN ODENDAAL

March, 23, 2020

I. SUMMARY

The purpose of the investigation is to implement a Boundary Element Methodology to analyze hydrodynamic phenomena on a custom created hull geometry and its associated response amplitudes. The analysis will consist of an introduction to the general theory of Panel Methods along with corresponding boundary conditions. This will be followed by an introduction to the model generation techniques and its parameters. Next, the necessary pre-processing steps will be discussed along with the associated Kelvin Wave Pattern. This analysis will focus on wave heights, pressures, and velocity vectors. Finally ship motion, Response Amplitude Operators, will be analyzed through the implementation of diffraction techniques. This study will conclude with a discussion on key learnings of viscous and non-viscous effects throughout the hydrodynamics analysis.

II. INTRODUCTION

Prediction of hydrodynamic forces due to ship motions is of extreme importance in ship design. The resistance experienced by the vessel is directly correlated to power and thus the overall fuel consumption. Therefore, to reduce these forces is an ever-important issue in hull design. Unfortunately, the accurate calculation of the wave patterns and the wave resistance of a ship has long-time proved difficult [1]. As such, The Boundary Element Method (BEM) has recently been developed and is currently the basis of many computational algorithms. Here the flow problem is solved using a simple potential model. Ultimately an investigation in the wave pattern and wave resistance using DELKELV and DELFRAC, in-house BEM programs, and a custom hull geometry is critically analyzed.

To successfully implement the BEM program DELKELV and DELFRAC, certain constraint conditions must be met. The ship Froude number must be less than 0.28. The geometry's waterline must be faired to a point, thus no transom can be present. The number of panels on the wet hull needs to be less than 500 panels. The draft-breadth ratio has to be more than 0.25. Finally, the geometry can not be a Wigley hull formulation.

III. GENERAL THEORY

i. Description of Potential Theory

The potential theory can be used to describe the velocity field in a fluid as the gradient of the velocity potential. Because of this, the potential flow is characterised by an irrotational velocity field:

$$\frac{\delta}{\delta \vec{x}} \times \vec{u} = \vec{0} \quad (1)$$

This formula then leads to the potential function. From this the velocity field can be determined which is the gradient of the potential function.

$$\frac{\delta \phi}{\delta x_i} = u_i \quad (2)$$

The potential function then needs to satisfy the Laplace-equation, given the fact that a potential flow will be incompressible:

$$\Delta \phi = \frac{\delta^2 \phi}{\delta x^2} + \frac{\delta^2 \phi}{\delta y^2} + \frac{\delta^2 \phi}{\delta z^2} = 0 \quad (3)$$

Finally it needs to be assumed that the flow is inviscid, since the flow will need to remain irrotational.

ii. Description of Boundary Conditions

For non-viscous flow models, as in DELKELV, the viscosity is zero which directly implies that it is possible for the fluid to flow at the surface of the flow domain without any shear forces. For the modelling of a vessel this results in a tangent flow along the surface with a tangential direction.

No leakage condition: Furthermore it is important that the "no leakage" condition is met, this means that no particles can appear or disappear on the surface. This means that the normal boundary condition that also applies for viscous flows is still valid, this can also be described in the following fomula:

$$\langle v_{flow}^{\vec{}} \cdot n_{surface}^{\vec{}} \rangle = \langle v_{surface}^{\vec{}} \cdot n_{surface}^{\vec{}} \rangle \quad (4)$$

The kinematic boundary condition: This condition means that at the free surface of the fluid the particles follow the free surface. This implies that particles cannot release itself from the free surface into the air, but also that particles do not move into the inner domain of the fluid.

The pressure boundary condition: Due to the change in wave height, the air pressure will also change due to a change in height. Furthermore there will be a pressure variation at the surface due to the changing velocity of the air. However since air is very light, these pressure changes are negligible and it is assumed that there is a constant pressure at the surface.

iii. The Panel Method

Numerical models which are based on potential flows, are known as BEM or Panel Methods. Ultimately, the basis of the panel method is that a very complex three-dimensional potential flow problem is converted to a simpler two-dimensional problem using Green's theorem:

$$\iiint_V (\nabla \Phi \cdot \nabla \Psi + \Phi \nabla^2 \Psi) dV = \iint_{\Omega} \Phi \nabla \Psi \cdot \vec{n} d\Omega = \iint_{\Omega} \Phi \frac{\delta \Psi}{\delta n} d\Omega \quad (5)$$

This 2D surface is thus composed of a distribution of sources and sinks, who's interactions can be solved at the boundaries to determine the velocities on the surface. This can be done using discretized surface panels and essential boundary conditions of tangential flows. DELFRAC is considered a panel method and it are based on the solution method of the 'von Neumann' conditions. This means, that the influence of the sources is expressed in velocity terms and that the normal boundary condition

at the surface of hull must be fulfilled. Where as, DELKELV is a panel method which incorporates ‘Dirchlet’ boundary conditions, where the model is based on potential flow.

IV. GEOMETRY DESCRIPTION

Before a BEM analysis can be completed, a hull must first be created. The motivation behind the hull creation comes from a traditional sailing yacht concept. It should be noted that the DELKELV program limitations on modern transoms, a rear point convergence was required. This posed some difficulties in modelling an exact sailing hull shape where transoms are typically included to improve overall stability. However, the ultimate goal was not to completely replicate a previous hull design, but to create a new distinct shape from which a thorough analysis and recommendations and learnings could be created.

Table 1: Hull Geometry Key Parameters

Ship Parameters		
Froude Number	F_n	0.28
Design Speed	$V(m/s)$	4.80
Length	$L(m)$	30.00
Breadth	$B(m)$	4.75
Draft	$T(m)$	2.25
Block Coeff.	C_B	0.37
Displacement	$\nabla(m^3)$	129.48
Metacentric Trans.	$GM_T(m)$	1.16
Metacentric Long.	$GM_L(m)$	45.57
Vertical COB	$COB_V(m)$	-0.75
Horizontal COB	$COB_L(m)$	15.63
Heave ω_{high}	$\omega_{high,heave}$ (Hz)	4.04
Roll ω_{high}	$\omega_{high,roll}$ (Hz)	3.56
Pitch ω_{high}	$\omega_{high,pitch}$ (Hz)	5.64

Model Generation To develop the hull as smoothly as possible, Bi-cubic Bezier surfaces were used. These type of curves are simply defined by a square grid and control points. The surface between the edges is controlled by a simple proportion of the nearby control points. As such, the wetted hull model was generated using two Bicubic Bezier surfaces which were then patched together to allow for a higher degree of surface control and panel reduction. Each patch can be defined using the following formulation,

$$S = \begin{pmatrix} (1-u)^3 & 3u(1-u)^2 & 3u^2(1-u) & u^3 \end{pmatrix} P \begin{pmatrix} (1-v)^3 \\ 3v(1-v)^2 \\ 3v^2(1-v) \\ v^3 \end{pmatrix} \quad (6)$$

Where P are the control points and u,v are the line spacing and line spacing transposed respectively. Using the above formulation the geometry was created for the analysis using MATLAB. To conserve computational demand, DELKELV automatically mirrors and encloses the ship hull, as such only half the surface is required to be modeled. The modelled geometry can be seen figure (10) and a summary of the key geometry parameters can be found in table (1).

V. DELKELV PRE-PROCESSING

To correctly utilize DELKELV, the appropriate, number of waves, panel sizes, and panel spacing techniques must be correctly im-

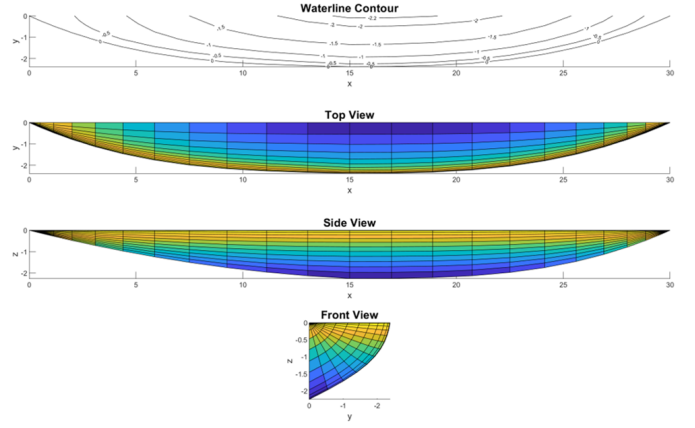


Figure 1: Wet Surface Lines and Shape. A larger figure can be found in the appendix.

plemented and established. A summary of the results can be seen in table (2).

i. Grids, Panels and Angles

Domain Length and Width To successfully obtain an appropriate wave pattern in the DELKELV, the domain must be appropriately established to ensure all phenomenon are captured in the results. A fair starting amount in front of the vessel is half the ships length. Since DELKELV is based on a Galileo transformation, the flow direction starts from left to right. Physically nothing happens before the vessel therefore computational demand can be conserved by issuing less grid panels. To establish a nice range after the vessel, the length of the domain can should be that of the length of the ship. This allows for a full development of the wave pattern with a complete domain length of $3L/2$. The width of the free surface domain can be determined using the Kelvin Wave Angle. This uses the assumption of a moving pressure point in still water with induces a predetermined angle of $19^\circ.28'$. Therefore, the wave pattern can fully be captured in two ship lengths and taking a half beam offset into account. Therefore the width of the domain can be approximately describe as,

$$W \geq 2L \tan(19.5^\circ) + B/2 \quad (7)$$

DELKELV Panel Size Generally ships operate with less than 4 waves per ship. To determine the number of waves present a relation between Froude number, wave lengths, and panel lengths can be used as follows,

$$n = 1/2 \pi F_n^2 \quad (8) \quad \lambda_{panel} = \lambda_{wave}/12 \quad (10)$$

$$\lambda_w = 2 \pi F_n^2 L \quad (9) \quad NP = L_{ship}/\lambda_{wave} \quad (11)$$

Using a Froude number of 0.28 it can be determined that 2 waves will appear. For a proper convergence of the wave pattern the panel ratio, $\lambda_{wave}/\lambda_{panel}$, should be around 12 when using DELKELV. This will allow for sufficiently small panel sizes to ensure the physics is fully captured. Therefore, the number of panels required will be the total length of the vessel divided by the length of the panels. This results in a total number of required panels of 24 in the longitudinal direction. The total number of panels on the half wetted hull surface are a 24x12 grid, resulting

in 288 total panels. This amount meets the required panel restriction of 500 panels. A complete summary can be found in table (2).

Wet Surface Cosine Spacing To ensure that the physics is properly captured at the points of stagnation, bow and aft cosine spacing of was applied on the wetted surface. The process will be done in the curvilinear plane. This means that the coordinates is a straight line in the curvilinear coordinate plane. As such the total length of the curve is spanned by a half circle. Then this circle is divided into a number of circular arcs of the same length. These circular arcs are then projected back on the plane, creating the panels in the wet surface. Mathematically this procedure can be represented as a unidirectional spacing starting from $L/2$,

$$\alpha_1 = \cos^{-1}(L/R) \quad (12) \quad \alpha = (i - 1)\alpha_{inc} + \alpha_1 \quad (14)$$

$$\alpha_{inc} = (\pi/2 - \alpha_1)/m \quad (13) \quad \delta S = R \cos(\alpha) \quad (15)$$

To ensure that the cosine spacing is appropriately applied and enlargement of the panels is not too large, a spacing factor between panel 1 and 2 of the starting edge was kept below 3. This allows for a smoother and less discontinuous analysis in the results. While, the cosine spacing was successfully applied, the difficulty lied in combining the technique with the geometry patches. The first attempt created an artificial mid-ship refinement where the patches met. As such, a unidirectional cosine spacing was applied to each patch to ensure the geometry only refined the fore and aft sections.

Free Surface Normal Spacing The free surface was broken into 3 sections, each corresponding to the individual domain lengths; front ($L/2$), middle (L), and aft (L). For each of these sections a constant normal spacing was applied and then combined to form the complete free surface. DELKELV does not require points on the wet and the free surface to coincide, however it does appear that the best results are obtained when the panels are maintained as square as possible. To ensure that the free surface points matched the contour of the geometry, a pseudo geometry was created with uniformly spaced coordinate points. Therefore, with a total domain length of 75m and width of 22m, the number of square cells in the free surface are 1080. The complete grid can be seen with the associated domain dimensions and flow directions in figure (2). While the uniform grid proved

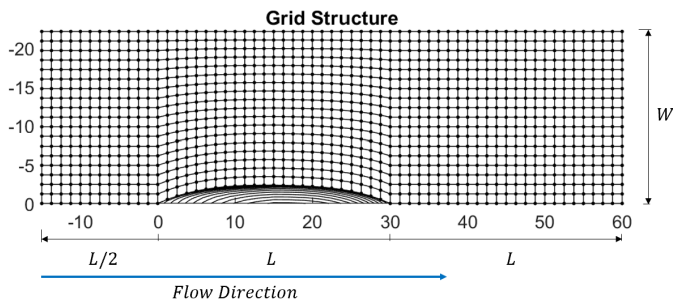


Figure 2: Complete domain, flow direction, and grid dimensions. A larger figure can be found in the appendix.

much more intuitive than the hull surface, one difficulty occurred

along the hull. This region, as seen in the figure, created a curved shape offset to each grid point. To fit the rectangular domain, this offset of points need to be scaled accordingly to gradually reduce curved effect. To achieve this, a ratio between the number of horizontal panels and spaces was required at each offset.

$$Scale = \frac{H_{panel} - i}{H_{panel}}$$

Where i , is the incremental number of grid points in the width direction.

Table 2: DELKELV Key Parameter Summary

Pre-Processing Parameters	
Number of Waves	2
Flow Direction	Left - Right
Wet Surface Spacing	Cosine
Free Surface Spacing	Uniform
Panel Length, λ_{panel}	1.23m
Panel Distribution	24 x 12
Wet Surface Panel #	288
Free Surface Panel #	1080

VI. ANALYSIS RESULTS DELKELV

After thoroughly determining the key input parameters, DELKELV was implemented to produce a corresponding wave pattern for the created geometry. Three parameters of interest are analyzed. The first is a 2D view of the kelvin wave pattern. This analysis, will reflect whether the estimated theoretical angle matches the output. The second analysis will consist of investigating the overall wave heights produced as seen from a birds perspective. The third analysis will investigate the pressures produced on the hull. This will be coupled with a tangential velocity vector analysis to get a better understanding of pressure gradients zones leading to velocity variations on the hull.

Top View Analysis As seen from the 2D outputs in figure (3) and (4) a clear wave pattern is produced. Along side of the vessel it can be seen that 2 wave lengths are produced. This matches the previous theoretical determination at the corresponding Froude number of 0.28. It can also be seen that the that theoretical Kelvin angle closely matches with what is displayed from the results. While there is some uncertainty in the measurement, the measured angle lies between 19° and 20° .

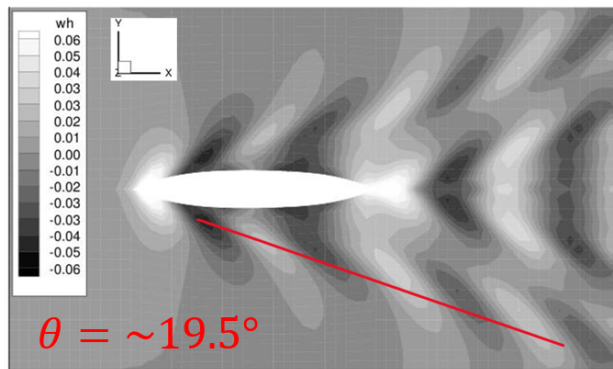


Figure 3: Monochrome kelvin wave pattern (wave height).

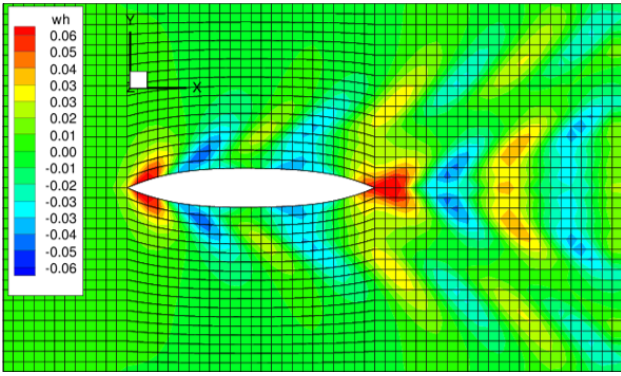


Figure 4: Monochrome Kelvin wave pattern (wave height x5). A larger figure can be found in the appendix.

Bird View Analysis After careful DELKELV post-processing, corresponding wave heights can be visually observed on the free surface grid. These results can be seen in both gray and colored figures (5) and (6). It can be viewed that the maximum wave height is close to 0.06m. While the minimum corresponds a negative 0.06m relative to the mean surface water level. It should be noted that the visual representation of the waves are magnified by a factor of 10 to visually see the results in the figures.

From the results it can be seen the largest wave heights correspond to both the bow and aft of the hull. It physically makes sense for large fore waves, as the vessel is propelling through the fluid at approximately 4.8m/s and a resulting wave will be induced. However, the stern of the vessel is an intriguing result. While a larger wave is to be expected, the magnitude in general is quite large. This may have to do with the potential flow model, where separation of the fluid does not occur. Thus the large stern wave may be over estimated due to the combined fluid summations being drawn to a rear point.

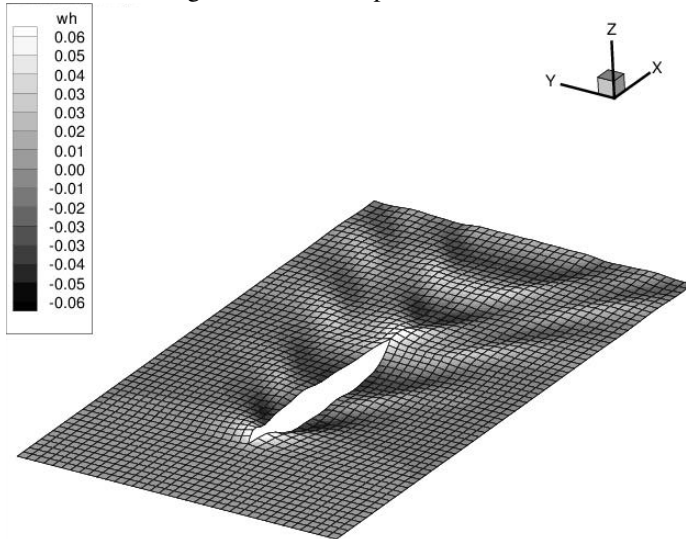


Figure 5: Monochrome Bird view (Wave Height x10). A larger figure can be found in the appendix.

Fish View Analysis When analyzing the pressures on the surface of the hull, a clear indication of high and low pressure

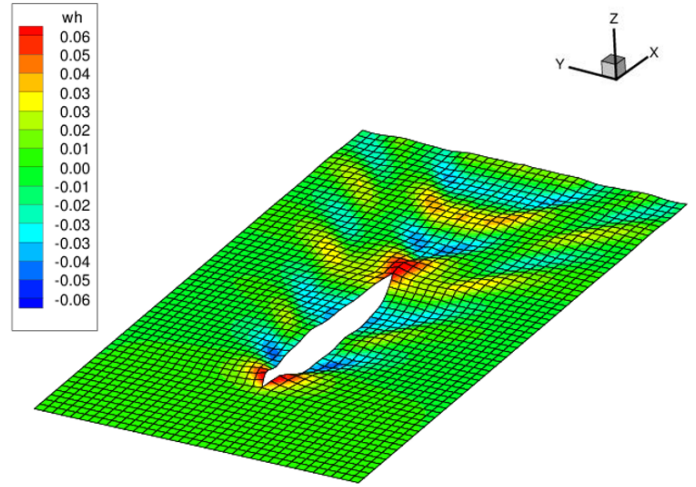


Figure 6: Color Bird view (Wave Height x10). A larger figure can be found in the appendix.

regions can be seen. The highest pressure regions correspond with the location of the highest wave heights. Since the model deals with potential non-viscous flows, stagnation pressures occur at the fore and aft of the hull. Whereas, the lower pressure regions correspond to the lows in the wave height. Therefore, the pressure region with the lowest pressure relates to a wet surface exposed to the ambient pressure. Pressure regions are also a strong indication of the fluid velocity over the hull surface. Thus, the largest pressure gradients on the wet surface correspond to a large velocity change. These velocity vectors can be seen in figure (8). This may give indication that the hull geometry curvature is inefficient and the flow of these regions are not uniformly distributed. One such region that may require further investigation occurs just aft of the midships. This region is engulfed in a low pressure region, which quickly transitions to high pressure region. This increasing pressure gradient physically causes velocity to slow very quickly, thus creating a higher region of fluid resistance against the hull.

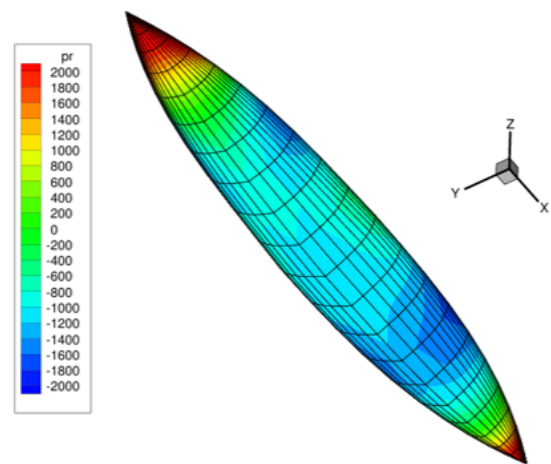


Figure 7: Color Fish View (Pressure).

i. Wave Amplitude Analysis

When a wave moves across the water surface, a point on the water describes a circular motion with a diameter equal to that of

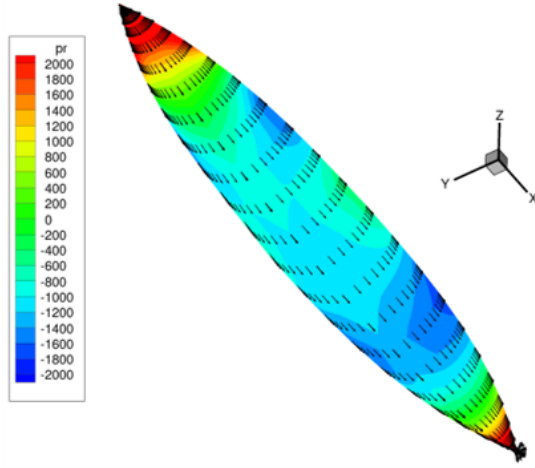


Figure 8: Color Fish View (Velocity and Pressure). A larger figure can be found in the appendix.

the wave height. This circular motion is also transmitted through, into the depth of the water. Typically a rule of thumb suggests that the water is disturbed up to a depth of about one-half of the wavelength, otherwise known as the wave base. In the analyzed case the total height of the maximum wave orbit is 0.12m. Thus the effect will be transmitted to an approximate depth of 7.4m, considering a total wavelength of 14.8m.

ii. Potential Analysis Restrictions

The following assessment of potential flow restrictions and limitations can be made when analyzing wave patterns using panel methods:

1. Potential-flow methods provide no information on the viscous flow. The velocity field computed contains no boundary layer or wake. Therefore, the pressure field is less affected. Also, flow separation is not indicated in the model.
2. The occurrence of a thick boundary layer reduces the pressure level at the stern. Also, sharp pressure rises at the stern are unlikely to occur in a viscous flow. These effects are disregarded in potential flow codes, which gives restrictions on their applicability. Specifically, it prevents making a quantitatively accurate prediction of the stern wave system for all but the most-slender vessels. In general, the amplitude of the stern wave system is overestimated by inviscid codes [1]
3. It is also not possible to make a quantitatively accurate prediction of the wave resistance for cases in which the stern wave system is substantially affected by viscous effects [1].

VII. SHIP MOTIONS

i. Frequency Range Analysis

Eigen Frequency Range Formula (16) and (17) are used to determine the highest needed circular frequency needed for the calculations, however note that these formula's exclude the damping and the added mass of the vessel.

$$\omega_{high} = 2\sqrt{\frac{\rho g A_w}{m}} \quad (16) \quad \omega_{high} = 2\sqrt{\frac{GM\rho g \nabla}{I_{ii}}} \quad (17)$$

Where I_{ii} is the mass moment of inertia for x, y, and z respectively. This term can be expressed in terms of the radii of inertia and the solid mass of the structure. For ships the radii of inertia can be approximated when the distribution of mass is unknown. [2]

$$\begin{aligned} I_{xx} &= k_{xx}^2 \cdot \rho \nabla & k_{xx} &= 0.22 \cdot L \text{ to } 0.28 \cdot L \\ I_{yy} &= k_{yy}^2 \cdot \rho \nabla & k_{yy} &= 0.30 \cdot B \text{ to } 0.40 \cdot B \\ I_{zz} &= k_{zz}^2 \cdot \rho \nabla & k_{zz} &= 0.22 \cdot L \text{ to } 0.28 \cdot L \end{aligned}$$

This gives a needed circular frequency of 4.04, 3.56 and 5.56 for respectively heave, roll and pitch. Including the (unknown) added mass and damping would result in a lower natural frequency, so the highest circular frequency from formula (16) and (17) will therefore be even higher than two times the real natural frequency of the vessel. Therefore this gives a very safe and conservative estimation of the frequency limit and it could even be stated that the calculations can be stopped at a lower frequency because the fast decrease of the depth influence and the small wave number.

DELFRAC Panel Sizing Using the frequency range limits that have been determined in the above paragraph, the appropriate panel sizing for DELFRAC can be calculated. This can be done using the dispersion relation (18) and the wavelength relation formula (19) to determine the shortest required panel size length to capture the corresponding ranges.

$$\omega^2 = g \cdot k \quad (18) \quad \lambda = \frac{2\pi}{k} \quad (19)$$

To be able to calculate the diffraction phenomena in a correct way, four panels per wave are needed when implementing DELFRAC. This gives a required panel length of 0.48m. A detailed summary of the DELKELV parameters can be seen in table (3).

Table 3: DELFRAC Key Parameter Summary

Pre-Processing Parameters	
Radii of Gyration, k_{xx}	7.50m
Radii of Gyration, k_{yy}	1.66m
Radii of Gyration, k_{zz}	7.50m
Panel Length, λ_{panel}	0.48m
Panel Distribution	60 x 8
Wet Surface Panel #	480

ii. RAO Analysis

In figure (9) all six RAO's calculated by DELFRAC can be seen. A corresponding analysis for the RAO of the roll, pitch and heave will be analysed as these proved to be the most important. It can clearly be seen that all peaks fit amply within the frequency range determined earlier in the 'frequency range analysis'.

Roll Analysis The damping in roll direction is normally partially caused by the generated waves which dissipate energy from the vessel as well as by viscous effects such as vortices and

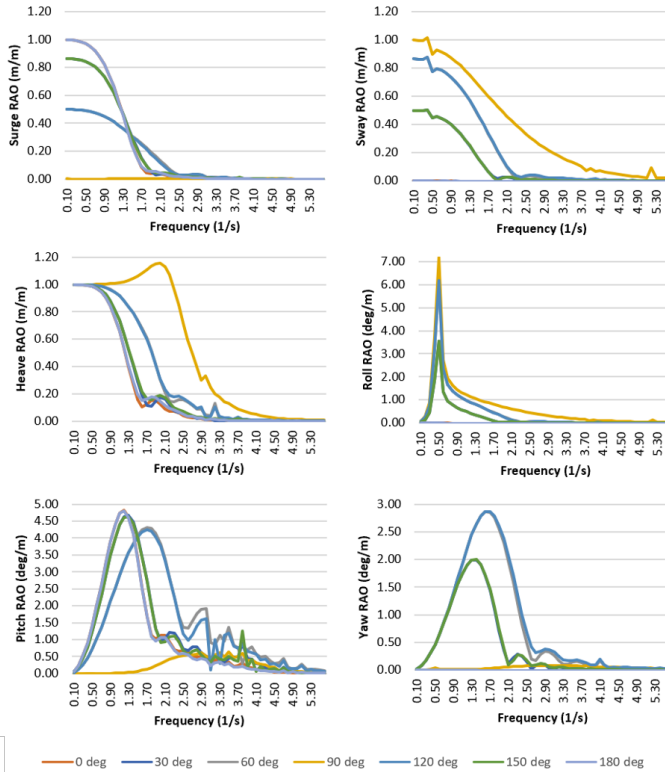


Figure 9: Response Amplitude Operators for varying wave angles. A larger figure can be found in the appendix.

skin friction. However the potential theory used by DELFRAC doesn't take into account these viscous effects which are usually significant in the roll motion while the damping by creating waves is less dominant in roll because of the round shape of the hull. In an extreme case with a circular cylinder, rotating about its center, it would not produce waves as its potential roll damping is zero. Altogether this results in a lack of damping which can also clearly be seen in the RAO of the roll direction in figure (9). Around the eigenfrequency a sharp-high peak can be seen in the response due to the lack of damping.

Heave Analysis The heave motions at zero forward speed in head waves at deep water are depicted as the orange line in figure 9. It can be seen that in very long waves (when $\omega \rightarrow 0$) the vessel will act like a buoy in the waves and will follow the wave surface (i.e. the heave amplitude will be equal to the wave amplitude). This results in a transfer function of 1 at low frequencies, which can be seen in the figure. At frequencies higher than the natural frequencies, it can be seen that the RAO decreases and finally that when the wave lengths are shorter than the ship length ($\omega > 1.43$), the transfer functions will tend to go zero[2]. In long beam waves (90 degrees, yellow line) the ship will behave like a buoy again and follows the surface and heave amplitude is equal wave amplitude so the RAO is 1. The difference with head waves is that with beam waves it is now the wave length to ship breadth ratio (L/B) that results in the behaviour of the ship. Therefore the heave motion behavior in beam waves is normally similar to the heave motion in head waves. However a higher resonance peak can be observed[2]. This can also clearly be seen again for the

RAO in the figure.

Pitch Analysis In extremely long waves (when $\omega \rightarrow 0$) the ship will behave again like a buoy and will follow the wave surface. Therefore the pitch amplitude will tend to be similar to the wave slope amplitude in long waves. Furthermore it can clearly be seen in the neighborhood of the eigenfrequencies resonance occurs, however at higher frequencies the pitch motions will again become very small. Also in beam waves the vessel has a response in pitch direction, which is caused by the anti-symmetry between the fore and aft body.

VIII. CONCLUSION

From the detailed analysis, it can be seen that using a panel method allowed for fast results for potential hull geometry optimization. However, difficulties and key learnings must be mentioned for future implementation.

The Boundary Element Methods produced results that were extremely fast relative to today's viscous solvers. This reduction in computational time proved to be extremely beneficial. However, non-viscous flow effects need to be fully understood prior to analysis to comprehend results and not misinterpret findings. One such area previously mentioned is in the resulting Rolling RAO. The spike peak produced is ultimately due to no damping and a smooth shaped hull being present, thus waves are not ample to dissipate the produced energy. Therefore the resulting motions are extremely large near the geometries natural frequency. Based on this effect, it can be inferred that other motions may also be slightly over-estimated.

Grid development also proved to be quite challenging. B-spline curves were used to develop the hull geometry with a cosine spaced grid. While this method proved to develop very smooth curves, the overall control of the panel number proved to be very difficult, since panel number is closely coupled in both length and height. Therefore, staying under the 500-panel restriction proved difficult. Another challenge with the hull grid generation was the overall control of the shape. While the hull could be freely changed to suit any shape, grid points produced irregularities when shapes produced large surface gradients. To improve upon this technique, it is suggested to implement multiple B-spline patches with a larger control net.

The recommended way to use these panel methods is through careful study of the wave pattern and pressure distribution and draw conclusions on possible hull form improvements from those. In general, it appears that for most practical cases, good results are obtained if enough care is given to the paneling and numerics. Therefore, provided that the restrictions are considered, and the results are sensibly considered, analyzed, and interpreted, potential flow codes can be very powerful and practical tools in ship design.

REFERENCES

- [1] Larsson, L. & Raven, H.C. (2010). *The Principles of Naval Architecture Series: Ship Resistance and Flow*. The Society of Naval Architect and Marine Engineers.
- [2] Journée, J.M.J. Massie, W.W. & Huijsmans, R.H.M. (2015). *Offshore Hydrodynamics. Third Edition* Delft University of Technology.

A. APPENDIX A: ALL FIGURES IN AN
ENLARGED FORMAT

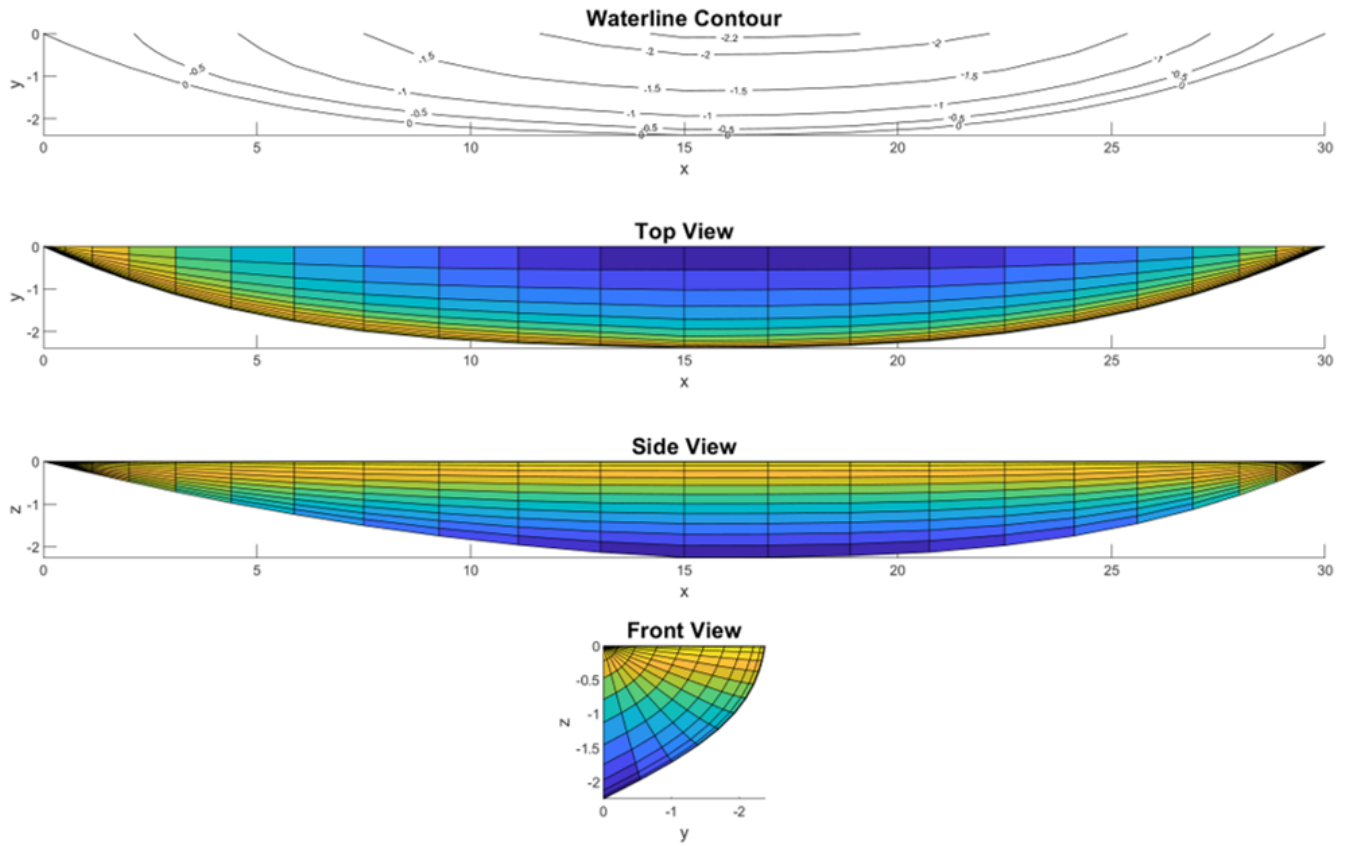


Figure 10: Wet Surface Lines and Shape

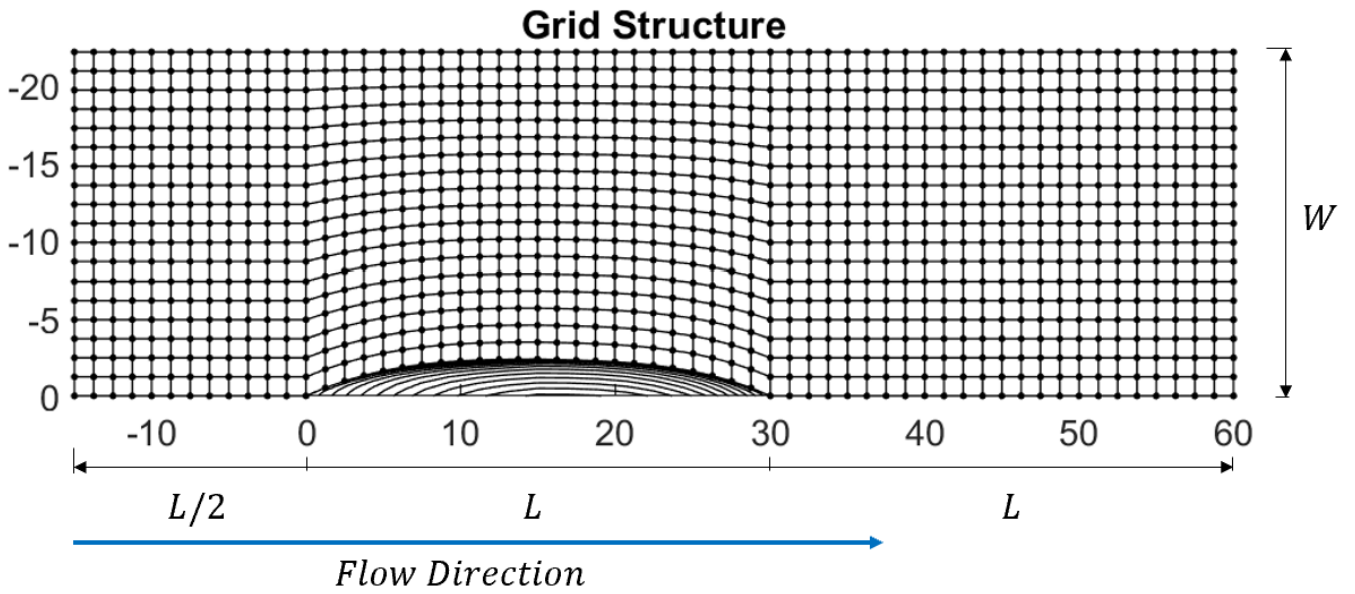


Figure 11: Complete domain, flow direction, and grid dimensions

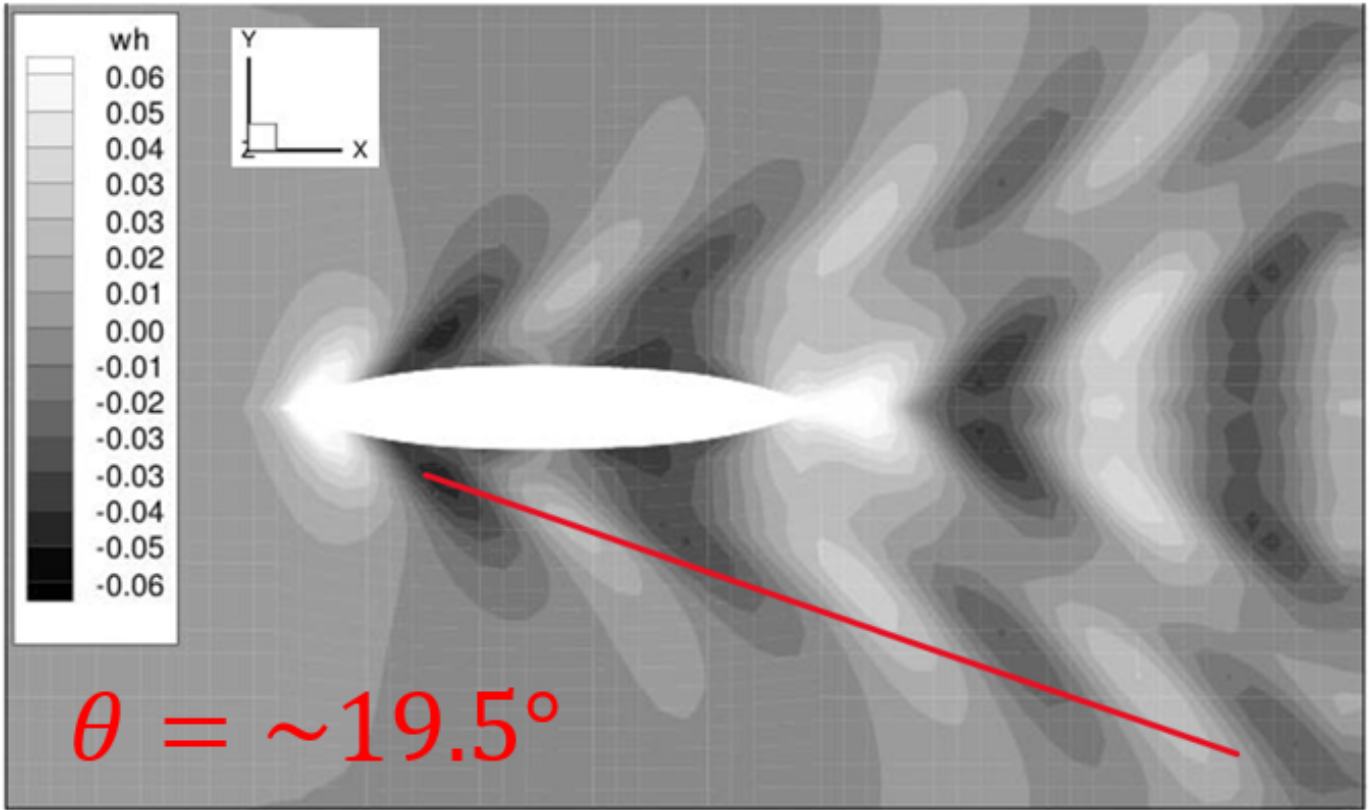


Figure 12: Monochrome kelvin wave pattern (wave height)

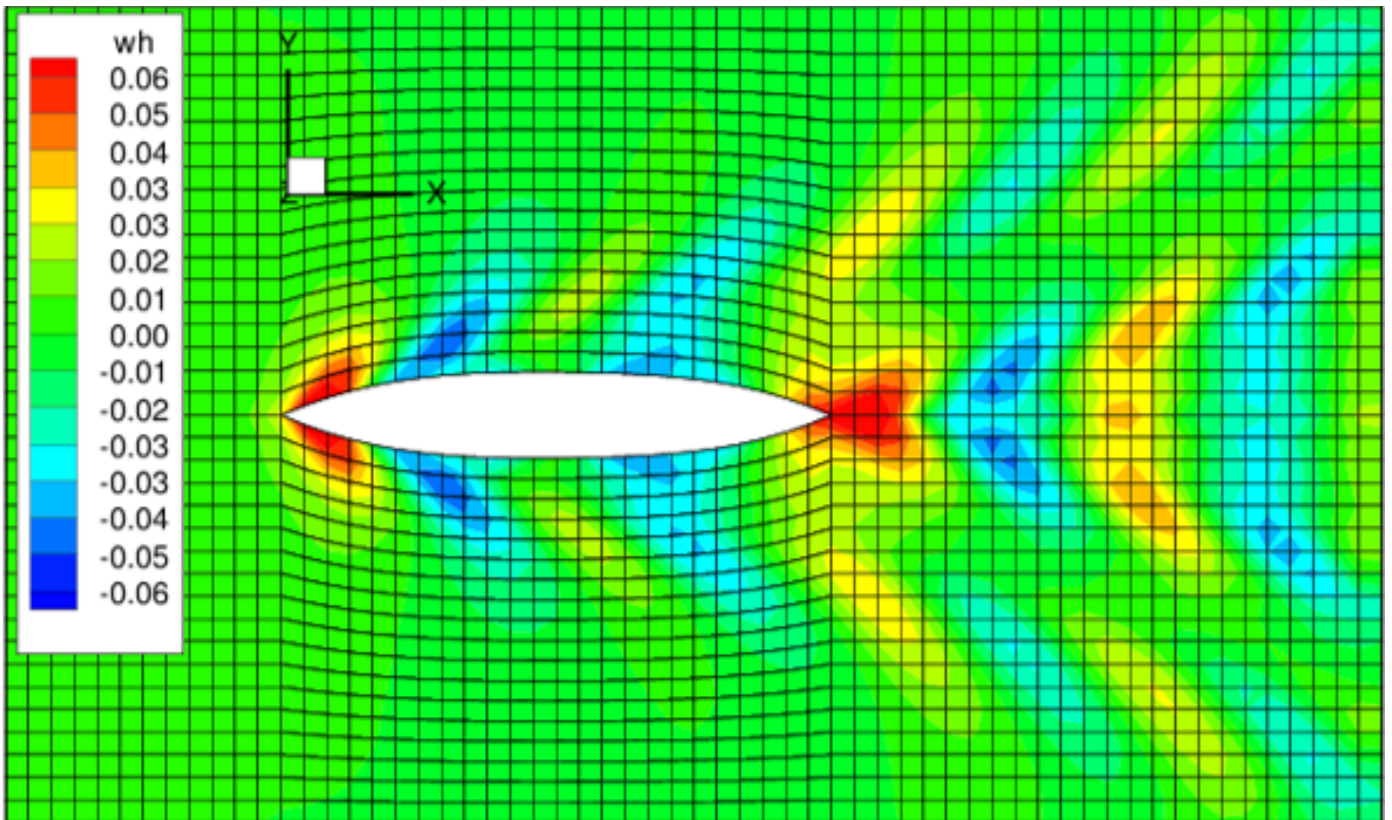


Figure 13: Monochrome kelvin wave pattern (wave height x5)

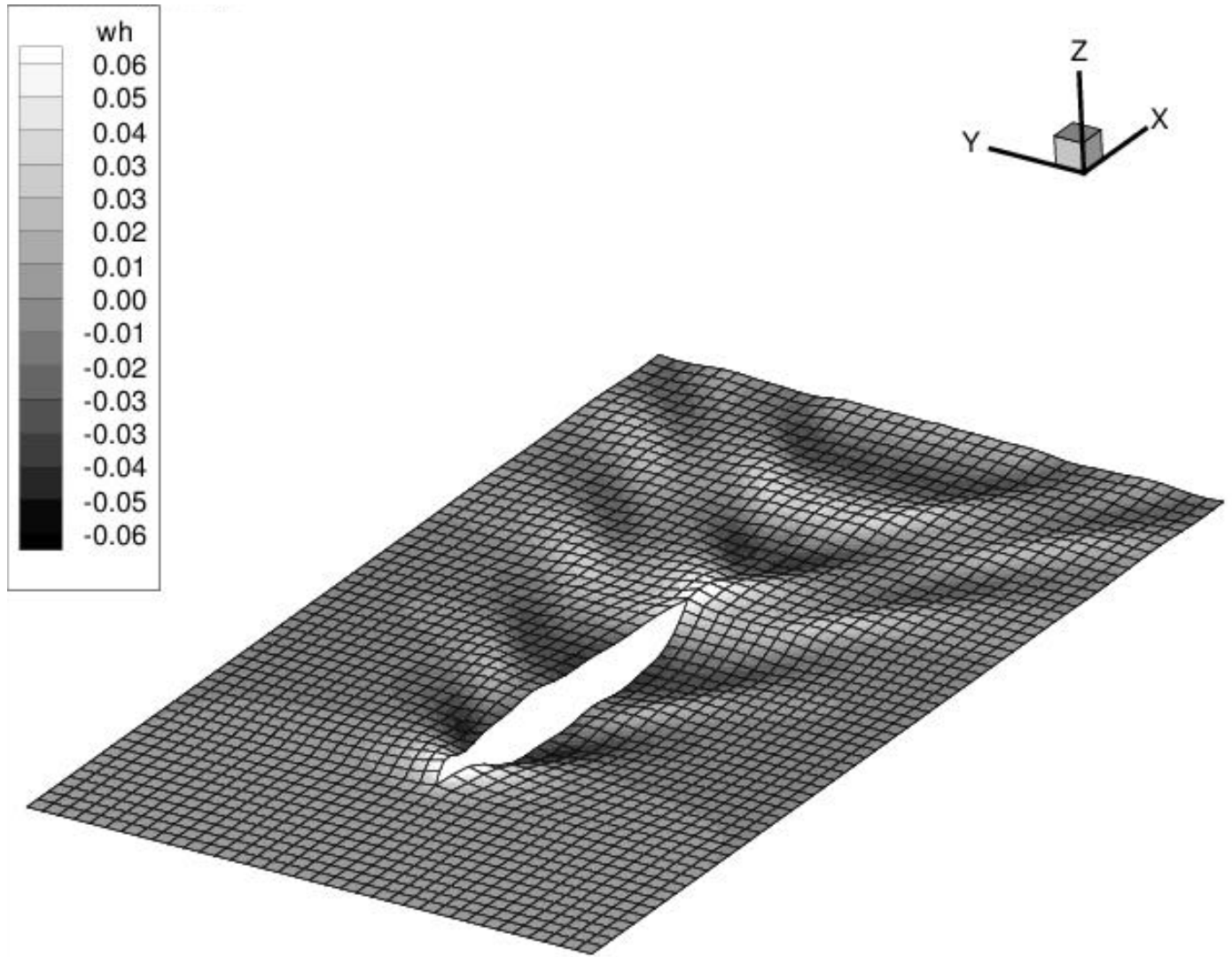


Figure 14: *Monochrome Bird view (Wave Height x10)*

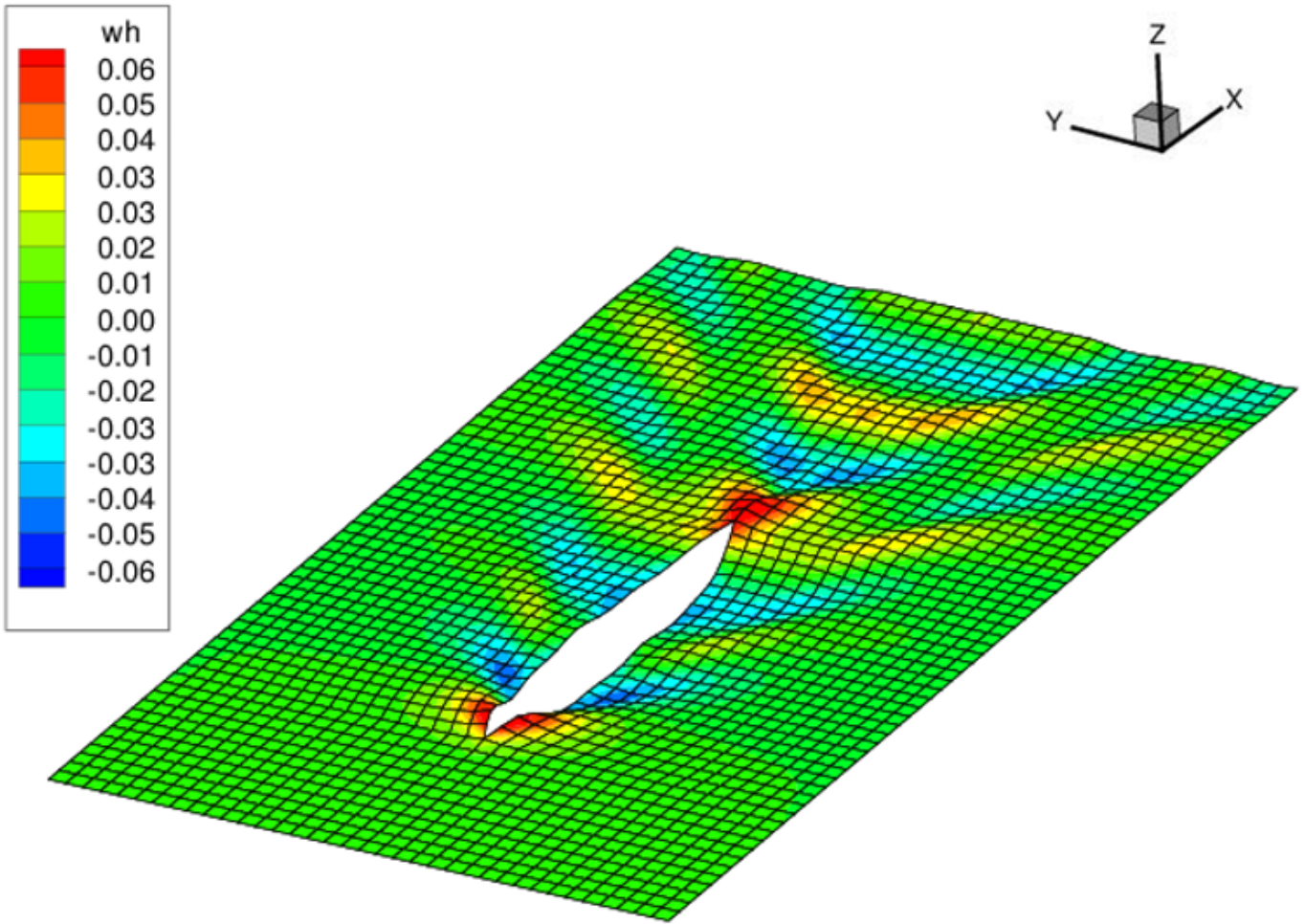


Figure 15: Color Bird view (Wave Height x10)

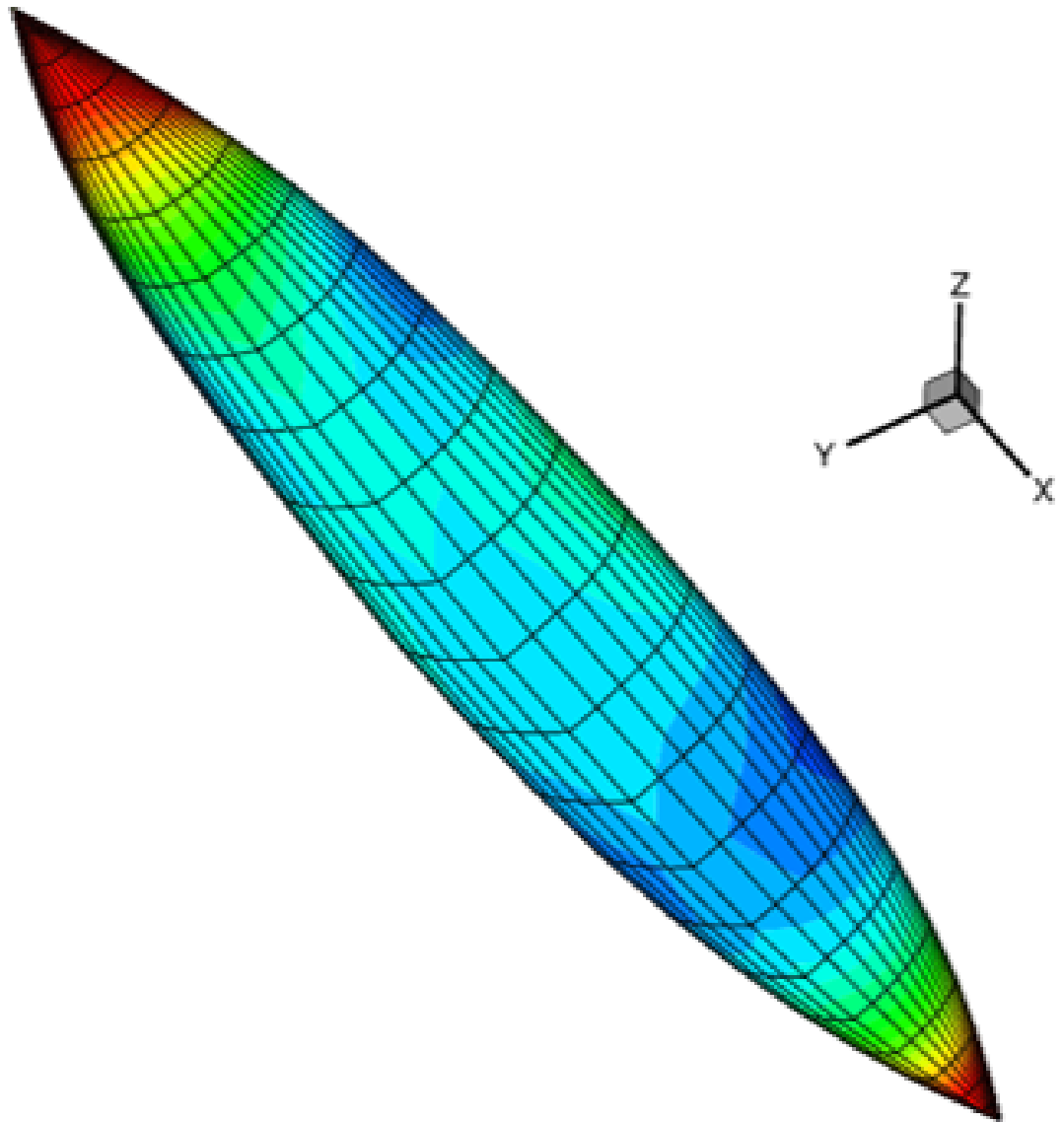
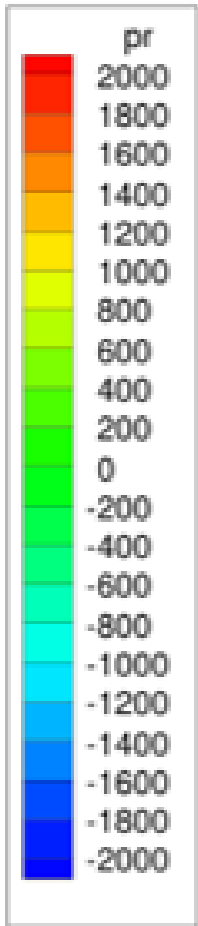


Figure 16: *Color Fish View (Pressure)*

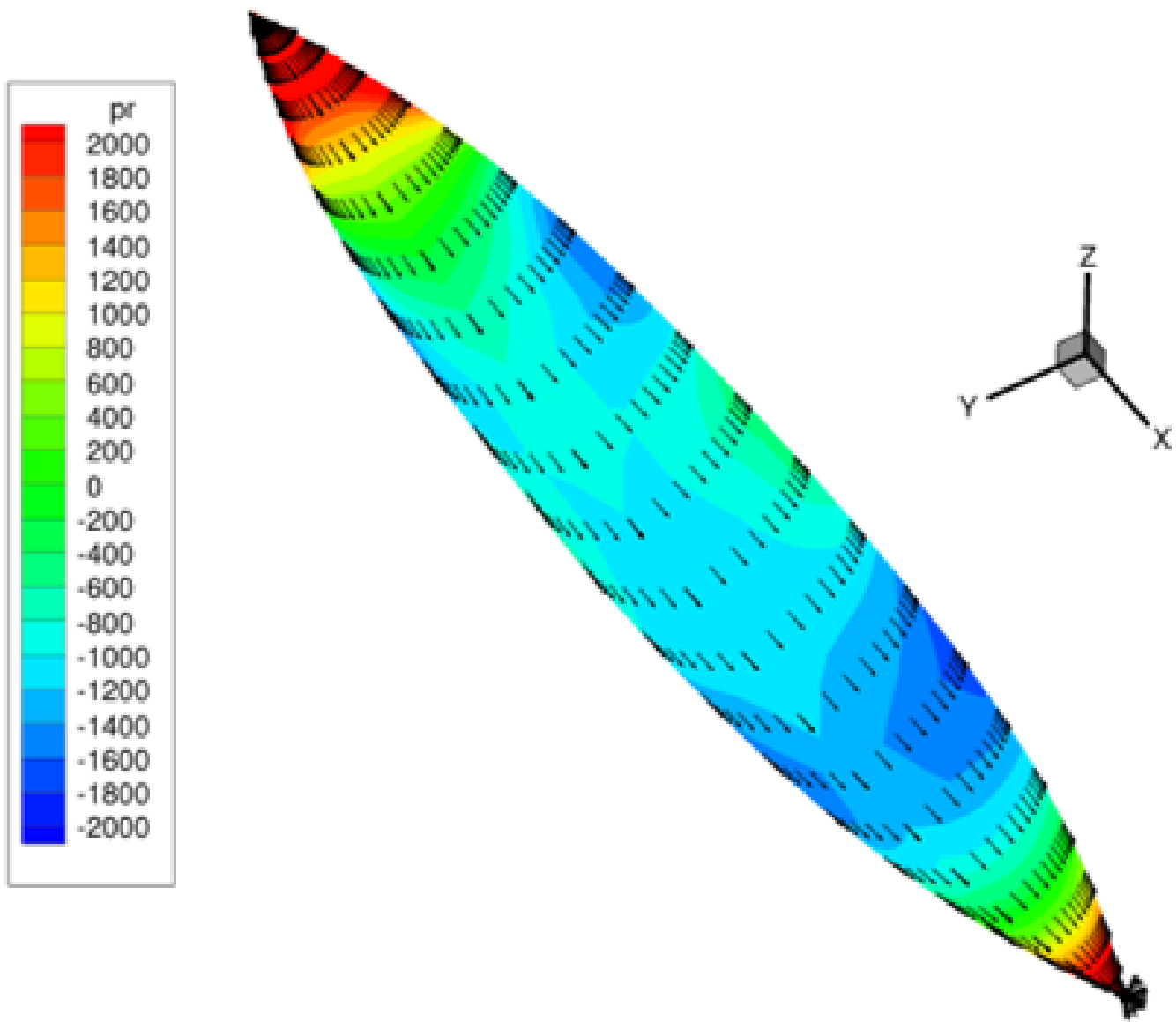


Figure 17: *Color Fish View (Velocity and Pressure)*

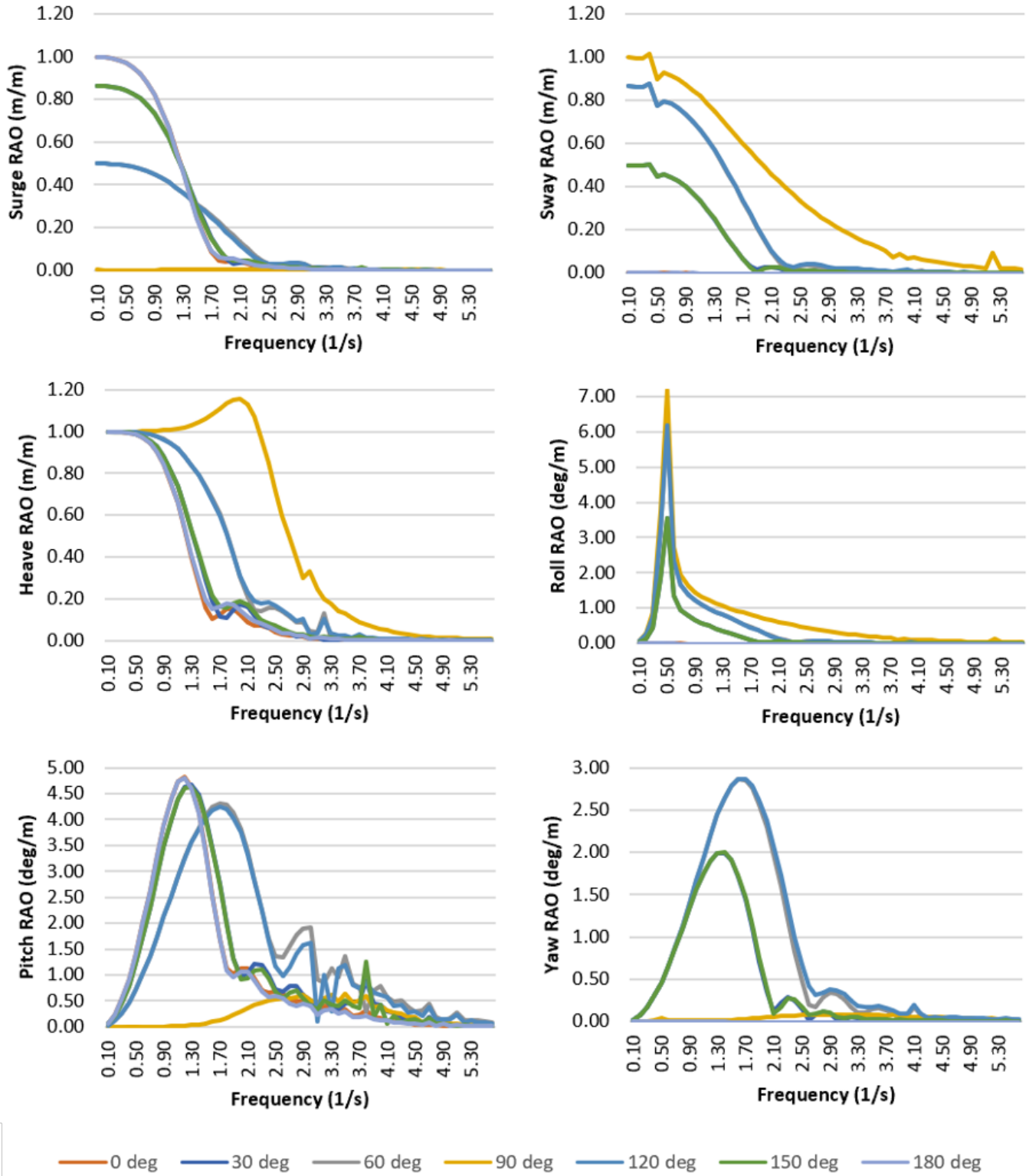


Figure 18: Response Amplitude Operators for varying wave angles